

## Infrared Optical Properties and Band Structure of $\alpha$ -Sn/Ge Superlattices on Ge Substrates

J. Olajos,<sup>(a)</sup> P. Vogl, W. Wegscheider, and G. Abstreiter

Walter Schottky Institut and Physik Department, Technische Universität München,  
D-8046 Garching, Federal Republic of Germany

(Received 6 May 1991)

Short-period  $\alpha$ -Sn/Ge strained-layer superlattices have been prepared on [001] Ge substrates by low-temperature molecular-beam epitaxy. We have achieved almost-defect-free and thermally stable single-crystalline structures. Photocurrent measurements in a series of  $\text{Sn}_1\text{Ge}_m$  ( $m > 10$ ) superlattices reveal a shift of the fundamental energy gap to smaller energies with decreasing Ge layer thickness  $m$ , in good agreement with band-structure calculations. A direct fundamental energy gap is predicted for a slightly increased lateral lattice constant in  $\alpha$ -Sn/Ge superlattices.

PACS numbers: 78.65.Gb, 71.25.Tn, 73.20.Dx

Band-structure engineering is one of the most fascinating aspects of modern semiconductor physics. The easiest way to change artificially the electronic structure of semiconductors is the formation of semiconductor alloys. This, however, leads to potential fluctuations due to the random occupation of lattice sites by different atoms. Alternatively, new man-made semiconductors with tailored band gaps may be achieved with short-period superlattices. So far, this idea has been pursued for various III-V compound semiconductor systems and also for Si/Ge which yield a limited range of energy gaps. Especially short-period strained-layer  $\text{Si}_n\text{Ge}_m$  ( $n$  and  $m$  denote the number of Si and Ge atomic planes in the unit cell, respectively) superlattices were studied extensively in the past few years because theory predicts that Brillouin-zone folding effects can lead to quasidirect energy gaps [1-5]. An unambiguous experimental identification of this effect, however, is still lacking. The combination of Si and Ge allows a band-gap variation between about 1.1 and 0.7 eV [6-8]. Within the group-IV semiconductors C, Si, Ge, and  $\alpha$ -Sn, the fundamental energy gap may be tuned, in principle, from 5.5 eV (diamond) down to 0 eV ( $\alpha$ -Sn). There exist, however, major problems in the experimental realization of various combinations of these materials which stem from the large lattice mismatch and the negligible solid solubility, especially for C and Sn. This applies particularly to random  $\text{Sn}_x\text{Ge}_{1-x}$  alloys even though they are expected to possess very interesting optical and electronic properties [9-12].

In the present communication we demonstrate that pseudomorphic, lattice-matched short-period strained-layer Sn/Ge superlattices (SLS's) can be realized experimentally. We have observed, for the first time, a dramatic shift of the fundamental band gap to smaller energies with increasing overall Sn concentration, in full agreement with our theoretical predictions. Band-structure calculations show, in addition, that these  $\alpha$ - $\text{Sn}_n\text{Ge}_m$  SLS's can have intrinsically direct energy gaps at  $\mathbf{k}=0$  which are not caused by a folding of electronic states into the superlattice Brillouin zone, in contrast to  $\text{Si}_n\text{Ge}_m$  SLS's [2,3].

In this Letter we report on the fabrication of almost-

defect-free and stable  $\alpha$ - $\text{Sn}_n\text{Ge}_m$  superlattices which have been grown by low-temperature molecular-beam epitaxy (MBE) on [001] Ge substrates. Photocurrent measurements show a systematic shift of the absorption onset to lower energies with decreasing Ge content in the SLS's. The observed shift agrees excellently with the theoretically predicted narrowing of the fundamental energy gap. For the Ge-substrate lateral lattice constant, this gap still remains indirect in  $\mathbf{k}$  space. Finally, we predict conditions which yield an intrinsic direct energy gap at  $\mathbf{k}=0$  with strong optical interband transition matrix elements. Importantly, we find this direct gap to be unrelated to the small-gap nature of  $\alpha$ -Sn.

Recently, several groups tried to grow  $\alpha$ -Sn or  $\alpha$ - $\text{Sn}_x\text{Ge}_{1-x}$  alloys by heteroepitaxy on various substrates [13-18]. The phase transition of Sn from the diamond-structure  $\alpha$  phase to the metallic body-centered-tetragonal  $\beta$  phase at  $T=13.2^\circ\text{C}$  causes Sn to be a difficult material to deal with. In films grown on diamond-structure substrates it has been shown that this transition temperature can be raised considerably [9]. No clear experimental evidence of a shift in the band gap of these Sn/Ge structures has been reported so far, however. We have used a new and unconventional technique to grow high-quality  $\alpha$ -Sn/Ge superlattices [19].

The multilayer structures were deposited in a special MBE system which allows strong temperature variations during growth. The layers were deposited far away from thermodynamic equilibrium conditions with a substrate temperature modulation between about 50 and  $300^\circ\text{C}$  during growth. Details of growth properties and growth conditions have been published elsewhere [19]. Here we focus on a series of samples which have been prepared under optimized conditions. They consist of 20 periods of  $\text{Sn}_1\text{Ge}_m$  ( $m=11, 15, \text{ and } 21$ ) superlattices which have been grown on [001] Ge and repeated four times with 700-Å Ge layers in between. These Ge buffer layers decrease the average lattice mismatch between the whole structure and the Ge substrate. Figure 1 shows a cross-sectional TEM bright-field image of a section of the nominally  $\text{Sn}_1\text{Ge}_{15}$  superlattice. The initially planar layering becomes slightly wavy at the end of the twenty periods,

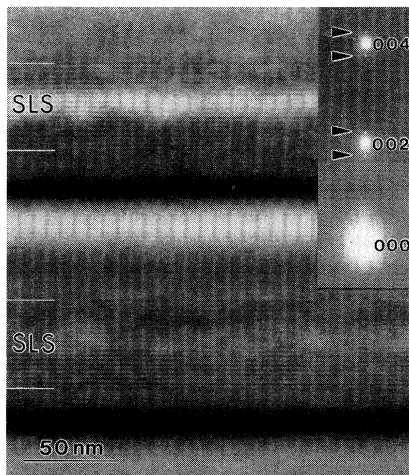


FIG. 1. Cross-sectional TEM bright-field image [ $g = (004)$ ] of the sample containing four 20-period  $\text{Sn}_1\text{Ge}_{15}$  SLS's. The selected-area diffraction pattern of the multilayer structure taken in the  $[110]$  zone axis is shown in the inset.

but becomes smooth again after the intermediate Ge layer. From detailed *in situ* Auger analysis and post-growth characterization by Raman spectroscopy and high-resolution TEM, we could extract a concentration profile of the superlattices. The concentration of Sn in the first atomic plane turns out to be approximately one-third of a monolayer, followed by an exponential decay and a negligible Sn content beyond a coverage of ten monolayers of Ge.

In order to get information on the fundamental band gap of these (SnGe)/Ge superlattices, we have performed infrared photocurrent measurements. Ohmic contacts were obtained by evaporating Ti/Sb/Au on the rectangular shaped cleaved samples and annealing for 30 s at  $T=320^\circ\text{C}$ . Care has been taken to avoid structural phase transformations of the Sn or the SnGe alloys which can be easily observed by optical inspection of the sample surface under a microscope. At the phase transition, the mirrorlike flat surface changes into a spotty surface [20]. We determined the transition temperatures to be 430, 450, and  $465^\circ\text{C}$  for  $\text{Sn}_1\text{Ge}_{11}$ ,  $\text{Sn}_1\text{Ge}_{15}$ , and  $\text{Sn}_1\text{Ge}_{21}$ , respectively. Photocurrent measurements were performed in the energy range 0.4 to 1.1 eV using a quartz-halogen light source together with a single-grating monochromator and filters. The samples were mounted in a He cryostat. The transmittance of the whole system was calibrated with a pyroelectric detector such that the measured photocurrent could be normalized to the incident photon flux. The samples were cooled to liquid-He temperatures in order to freeze out the holes in the epitaxial Ge layers which turned out to be unintentionally boron doped due to the boron nitride crucibles used in our low-temperature MBE system. In addition to the superlattice samples, we also measured the photocurrent of a Ge reference sample which was grown under the same conditions.

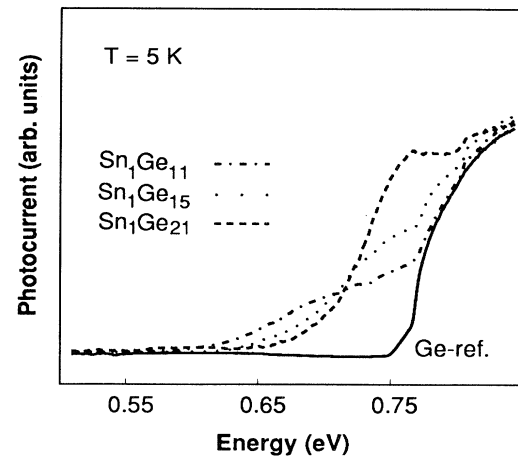


FIG. 2. Photocurrent vs photon energy for the Ge reference sample and the various  $\text{Sn}_1\text{Ge}_m$  strained-layer superlattices.

Figure 2 shows the raw photocurrent spectra of the four samples in the energy range of 0.5 to 0.8 eV. In the Ge reference sample, we have observed a strong signal above 0.75 eV due to interband electron-hole excitations. Also, the onset of phonon-assisted transitions has been observed. The photocurrent spectra of the superlattices exhibit, in addition, a strong signal below the Ge band gap whose onset is clearly shifted to smaller energies with decreasing Ge concentration. For a given photon flux, the photocurrent is proportional to the absorption coefficient  $\alpha$ , provided the absorbing layer is much thinner than  $\alpha^{-1}$ . This condition is expected to be fulfilled in our samples for photon energies below the Ge band gap. Therefore we have converted the photocurrent below 0.75 eV into the absorption coefficient. Figure 3 shows the relative change of  $\alpha$  versus energy as obtained from such a normalization procedure for the three superlattice samples. The absorption edge is rather smooth and shifts roughly from 0.66 eV for  $\text{Sn}_1\text{Ge}_{21}$  to 0.56 eV for  $\text{Sn}_1\text{Ge}_{11}$ . The arrows underneath each of the experimental curves in Fig. 3 mark the theoretically predicted energy gaps, as obtained from superlattice band-structure calculations which are discussed below. In particular, the black arrows correspond to the calculated fundamental energy gap for perfectly sharp SLS's. It is indirect in  $\mathbf{k}$  space. The gray arrows mark the predicted energy gaps of smeared concentration profiles. As mentioned before, the actual samples have a compositional profile somewhere in between these two extreme cases. The positions of the absorption edges and their shift with the Ge content are in very good agreement with the calculated energy gaps. The smooth onset and the relative increase of the absorption coefficient is also consistent with the indirect nature of the fundamental energy gap as predicted by the present theory. We note, however, that overall confinement effects due to the relatively small number of repeated superlattice cells within the 700-Å Ge buffer layers

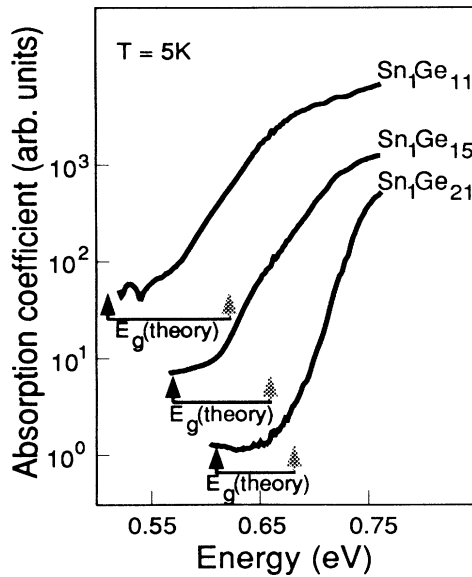


FIG. 3. Absorption coefficient below 0.75 eV as extracted from the normalized photocurrent data. The black and gray arrows mark the theoretically predicted indirect energy gap of the strained-layer superlattices with sharp interfaces and random alloys, respectively.

will also somewhat influence the exact position of the absorption edge.

The present calculations indicate that the electronic structure of  $\alpha$ - $\text{Sn}_n\text{Ge}_m$  SLS's is controlled by a unique interplay between very large strain effects, spin-orbit interaction effects, and quantum confinement of electronic states. Since the  $\alpha$ - $\text{Sn}_n\text{Ge}_m$  SLS's are grown pseudomorphically on [001] Ge, the Sn layers have a lateral lattice constant  $a_{\parallel} = a_{\text{Ge}} = 5.65 \text{ \AA}$ . This compression corresponds to a lateral strain of approximately 13% in the Sn layers. For tetragonally distorted pure  $\alpha$ -Sn layers, we obtain a lattice constant normal to the planes of  $a_{\perp} = 7.204 \text{ \AA}$  from simple elasticity theory. We have used this value for the strained Sn-Sn bonds and an arithmetic average of the strained Sn-Sn and Ge-Ge bond lengths for the Sn-Ge bonds in the SLS's, respectively. We have calculated the electronic structure of  $\alpha$ -Sn/Ge superlattices employing the empirical, nonlocal relativistic pseudopotential method of Chelikowski and Cohen [21] and generalizing it to superlattices. This generalization amounts to a smooth interpolation and volume renormalization of the bulk pseudopotential form factors for the simple tetragonal supercell and introduces no additional parameters. We have extensively tested our calculations by applying it to  $\text{Ge}_n\text{Si}_m$  SLS's. Our results compare very well with the gap-adjusted local-density-functional calculations of Refs. [2,3].

Unstrained bulk diamond-type  $\alpha$ -Sn ( $a = 6.498 \text{ \AA}$ ) is known to have a zero gap at  $\mathbf{k} = 0$  [9]. The present pseudopotential calculations predict that laterally compressed (i.e., tetragonal)  $\alpha$ -Sn with  $a_{\parallel} = a_{\text{Ge}}$  has a metallic ground

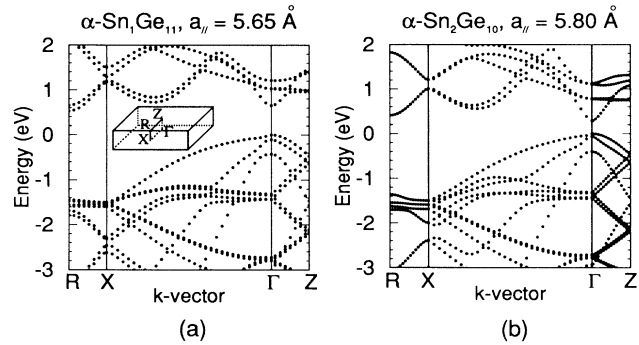


FIG. 4. Calculated band structure of (a) a  $\alpha$ - $\text{Sn}_1\text{Ge}_{11}$  superlattice with a lateral lattice constant  $a_{\parallel} = 5.65 \text{ \AA}$  and (b) a  $\alpha$ - $\text{Sn}_2\text{Ge}_{10}$  superlattice with  $a_{\parallel} = 5.80 \text{ \AA}$ . The superlattice Brillouin zone is shown schematically in the inset of (a).

state. Whereas the [001] strain opens a gap at  $\mathbf{k} = \Gamma$ , the conduction bands at the  $R$  point [for an unstrained twelve-layer superlattice, this corresponds to the  $L$  point in the fcc structure] are shifted downwards to an energy of  $-0.4 \text{ eV}$  below the Fermi energy. This implies that a single heterostructure consisting of a half-infinite Ge crystal and a laterally-lattice-matched half-infinite  $\alpha$ -Sn crystal is metallic and has no energy gap.

In a short-period superlattice, however, the quantum-mechanical confinement of the electronic states in the few Sn layers of the superlattice causes the Sn-related conduction bands at  $R$  and  $\Gamma$  to rise above the Ge-related conduction-band-edge states. Consequently, we find that there is a positive gap in the series of short-period SLS's  $\alpha$ - $\text{Sn}_n\text{Ge}_m$  with  $n < m/2$ .

An analysis of the electronic charge density reveals that the conduction-band states at  $R$  and  $\Gamma$  are purely Ge-like antibonding states which are strongly confined to the Ge layers. These states continuously evolve from the folded Ge band-edge states (i.e., from Ge in the Brillouin zone of  $\alpha$ - $\text{Sn}_0\text{Ge}_{n+m}$ ) without any band crossings. The valence-band states at  $\Gamma$ , on the other hand, are  $p$ -type bonding states built from the atomic Ge and Sn states in proportion to the relative concentration of Ge and Sn.

To compare with our experimental data, we have performed detailed calculations of  $\alpha$ - $\text{Sn}_1\text{Ge}_n$  superlattices with  $n = 3, 7, 11, 15, 19$ . In these cases, we find the top of the valence band at  $\Gamma$ , and the bottom of the conduction band at  $R$ . This indirect band gap increases with increasing  $n$  but approaches the value of bulk Ge very slowly. The calculations indicate that the conduction-band-edge state at the  $\Gamma$  point lies energetically above the state at  $R$  by  $0.16 \text{ eV}$ , nearly independent of the value of  $n$ . Figure 4(a) shows the calculated band structure of a  $\alpha$ - $\text{Sn}_1\text{Ge}_{11}$  SLS. The superlattice Brillouin zone is also shown. To account for the interface mixing, we have also calculated the electronic structure of smeared Sn profiles, employing the virtual crystal approximation. The calculations predict a small increase of the energy gap with intermixing, as indicated in Fig. 3 with the black and gray arrows.

According to the present theory, it is, however, also possible to produce a direct energy gap in  $\alpha$ -Sn $_n$ /Ge $_m$  SLS's with strong interband optical transition matrix elements just by slightly increasing the lateral lattice constant. A lateral lattice constant larger than  $a_{\text{Ge}}$  leads to a biaxial expansion—and consequently also to a hydrostatic expansion—of the Ge layers. Analogously to most semiconductors, a *hydrostatic* expansion yields a decrease of *all* conduction bands, with a decrease at  $\mathbf{k}=\Gamma$  being 3 times larger than at  $\mathbf{k}=R$  (this  $\mathbf{k}$  point corresponds to  $\mathbf{k}=L$  in cubic fcc structures). Since we find superlattice conduction- and valence-band-edge states to be predominantly Ge-like, as discussed above, we find that already a slight increase of  $a_{\parallel}$  produces an intrinsically direct energy gap at  $\mathbf{k}=0$  for a wide range of  $\alpha$ -Sn $_n$ Ge $_m$  SLS's with  $n < m/2$  and  $a_{\parallel} > a_{\text{Ge}}$ . The  $\alpha$ -Sn $_2$ Ge $_{10}$  superlattice, for example, is direct for  $5.7 \text{ \AA} < a_{\parallel} < 6.0 \text{ \AA}$ . This is shown in Fig. 4(b) for  $a_{\parallel} = 5.80 \text{ \AA}$ . This figure effectively shows the conversion of Ge, embedded in a SLS with very few Sn layers, into a crystal with an InSb-like band structure. We emphasize that this direct gap is primarily caused by the lateral strain of Ge and not by the small Sn band gap. On other hand, our calculations also predict that pure Ge always remains indirect for any strain so that Sn plays a secondary but subtle role in creating this new direct-gap group-IV semiconductor. We are currently trying to optimize MBE growth conditions with materials such as InP as the substrate in order to verify these predictions.

This work was supported by the Deutsche Forschungsgemeinschaft, project SFB No. 348.

<sup>(a)</sup>Permanent address: Department of Solid State Physics, University of Lund, S-221 00 Lund, Sweden.

[1] S. Froyen, D. M. Wood, and A. Zunger, Phys. Rev. B **37**, 6893 (1988).

[2] S. Satpathy, R. M. Martin, and C. G. van de Walle, Phys.

Rev. B **38**, 13237 (1988).

- [3] U. Schmid, N. E. Christensen, M. Alonani, and M. Cardona, Phys. Rev. B **43**, 14597 (1991).
- [4] P. Friedel, M. S. Hybertsen, and M. Schlüter, Phys. Rev. B **39**, 7974 (1989).
- [5] J. Morrison, M. Jaros, and K. B. Wong, Phys. Rev. B **35**, 9693 (1987); M. A. Gell, Phys. Rev. B **37**, 7535 (1988).
- [6] D. V. Lang, R. People, J. C. Bean, and A. M. Sergent, Appl. Phys. Lett. **47**, 1333 (1985).
- [7] T. P. Pearsall, J. Bevk, J. C. Bean, J. Bonar, and J. P. Mannaerts, Phys. Rev. B **39**, 3741 (1989).
- [8] R. Zachai, K. Eberl, G. Abstreiter, E. Kasper, and H. Kibbel, Phys. Rev. Lett. **64**, 1055 (1990).
- [9] C. H. L. Goodman, IEEE Proc. **129**, 189 (1982).
- [10] D. W. Jenkins and J. D. Dow, Phys. Rev. B **36**, 7994 (1987).
- [11] S. Groves and W. Paul, Phys. Rev. Lett. **11**, 194 (1963).
- [12] W. Wegscheider, K. Eberl, U. Menczigar, J. Olajos, G. Abstreiter, P. Vogl, in *Proceedings of the Twentieth International Conference on Physics of Semiconductors*, edited by E. M. Anastassakis and J. D. Joannopoulos (World Scientific, Singapore, 1990), p. 1685.
- [13] R. F. Farrow, D. S. Robertson, G. M. Williams, A. G. Cullis, G. R. Jones, I. M. Young, and P. N. J. Dennis, J. Cryst. Growth **54**, 507 (1981).
- [14] J. L. Reno and A. L. Stephenson, Appl. Phys. Lett. **54**, 2207 (1989).
- [15] M. T. Asom, A. R. Kortan, L. C. Kimerling, and R. C. Farrow, Appl. Phys. Lett. **55**, 1439 (1989).
- [16] S. J. Shak, J. E. Greene, L. L. Abeles, Q. Yao, and P. M. Raccah, J. Cryst. Growth **83**, 3 (1987).
- [17] R. P. Pukite, A. Harwit, and S. S. Iyer, Appl. Phys. Lett. **54**, 2142 (1989).
- [18] H. Höchst, M. A. Engelhardt, and J. Hernández-Calderón, Phys. Rev. B **40**, 9703 (1989).
- [19] W. Wegscheider, K. Eberl, U. Menczigar, and G. Abstreiter, Appl. Phys. Lett. **57**, 875 (1990).
- [20] J. Piao, R. Beresford, T. Licata, W. I. Wang, and H. Homma, J. Vac. Sci. Technol. B **8**, 221 (1990).
- [21] J. R. Chelikowski and M. L. Cohen, Phys. Rev. B **14**, 556 (1976).

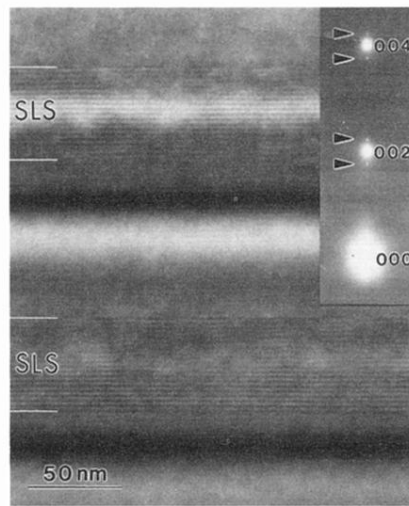


FIG. 1. Cross-sectional TEM bright-field image [ $g = (004)$ ] of the sample containing four 20-period  $\text{Sn}_1\text{Ge}_{15}$  SLS's. The selected-area diffraction pattern of the multilayer structure taken in the  $[110]$  zone axis is shown in the inset.